

P. TZALLAS<sup>1</sup>  
K. WITTE<sup>1</sup>  
G.D. TSAKIRIS<sup>1</sup>  
N.A. PAPAIOGIANNIS<sup>2</sup>  
D. CHARALAMBIDIS<sup>2,✉</sup>

## Extending optical fs metrology to XUV attosecond pulses

<sup>1</sup> Max-Planck-Institut für Quantenoptik, 85748 Garching, Germany

<sup>2</sup> Foundation for Research and Technology – Hellas, Institute of Electronic Structure & Laser, P.O. Box 1527, 711 10 Heraklion (Crete), Greece and Univ. of Crete Heraklion (Crete), Greece

Received: 2 September 2003/Accepted: 4 February 2004

Published online: 23 June 2004 • © Springer-Verlag 2004

**ABSTRACT** We report on the progress towards a 2nd-order autocorrelation measurement of a coherent superposition of the 7th to the 15th harmonic of the fundamental frequency of the Ti : Sapphire laser. The two-photon ionization of He atoms was investigated and found to be an appropriate non-linear detector. In addition, the technique of volume autocorrelation based on a split mirror wavefront divider was analysed and shown to exhibit adequate degree of modulation. Moreover, the approach presented opens up the path to XUV-pump XUV-probe type of temporal studies of ultrafast processes with a sub-fs temporal resolution.

PACS 42.60.By; 42.65.Re; 42.65.Ky

### 1 Introduction

Optical pulse engineering has succeeded in strikingly decreasing the laser pulse duration from a few picoseconds down to a few femtoseconds [1] over the last twenty years, thus providing a unique tool for the time domain study of a large number of ultra-fast processes. Several other processes, however, occur within characteristic times of one femtosecond or even shorter. Some typical examples of such processes are: i) the evolution of non-stationary quantum state superpositions in atoms and molecules; ii) the decay of electronic or dissociative states; iii) electron–electron correlation effects in atoms and molecules, in conjugation with aromatic rings or organic macromolecules, in quantum confined systems such as quantum wells and quantum dots, in superconductivity; iv) the dynamics of electron–electron scattering in semiconductors; and v) the early stages of energy redistribution in antenna complexes within the photosynthetic reaction center. Time domain studies of such processes require non-linear approaches and devices with sub-femtosecond temporal resolution. Significant steps towards this goal have recently been made by several research groups active in the fields of attosecond pulse engineering and metrology.

According to the superposition principle in wave mechanics, spatial or temporal energy localization comes about

whenever mutually coherent waves are superimposed in time and space. In particular a superposition of monochromatic light waves of equally spaced and properly phased frequencies results into a temporal beating, on which short pulse train generation [2–4] is based on. In this context, the harmonic emission from atoms appears to be a most suitable candidate for the temporal localization of light to unprecedented short time scales. Indeed in the two main approaches, utilized so far for the generation of attosecond pulses, the underpinning process is harmonic generation from atoms. The first approach uses laser pulses of a few optical cycles aiming at the generation of isolated attosecond pulses [5, 6], while in the second approach many-cycle laser pulses are exploited for the production of attosecond pulse trains [7, 8].

In the semi-classical description [9] and its extension to a full quantum theory [10, 11] of the interaction of an intense low frequency laser pulse with atoms, the combined oscillating potential of the atom and electric field of the laser pulse forms a local barrier that a single active bound electron can tunnel through or escape over. Subsequently, the almost free electron moves classically in the continuum gaining energy under the influence of the external laser field. Those electrons that return to the vicinity of the parent ion, which acts as a third body, may recombine to emit radiation with high energy and frequencies the harmonics of the driving laser field. The energy that the electron can gain from the field and the corresponding trajectory in the continuum depend sensitively on the phase of the field at the time of ionization. Speaking in terms of Feynman's path integrals, the harmonic spectrum results from the contributions of a number of interfering quantum paths describing the electron trajectories that lead to recombination [11]. In this spectrum, which consists of a series of equally spaced peaks around the frequencies of the odd harmonic of the fundamental as a consequence of the spherical symmetry of the atomic potential and the periodicity in the motion of the driven electron, two main regions are relevant to the two approaches utilized for attosecond pulse generation: a) the “cut off” region around the maximum emitted photon energy, that corresponds to the highest energy with which the electron may recombine, following one specific trajectory. The emitted intensity drops rapidly at energies higher than the cut off energy given by [10]  $\hbar\omega_{\max} = 3.17U_p + I_p \cdot F(I_p/U_p)$ , where  $U_p = e^2 E_L / 4m\omega_L^2$  is the average (ponderomotive) energy of the electron in the laser field  $E_L$ , and the

✉ Fax: +30-2820391318, E-mail: chara@iesl.forth.gr

function  $F(I_p/U_p)$ , which is due to electron tunnelling and diffusion effects has values close to unity and is usually ignored, following the semi-classical treatment; b) the “plateau region” at photon energies below  $\hbar\omega_{\max}$  consisting of a “comb” of approximately equal intensity peaks.

Part of the cut-off spectral region, is used for isolated attosecond pulse generation in the few-cycle laser pulse approach [12–16]. This emission of this spectral region occurs only during a small fraction of the optical cycle with the highest amplitude within the optical pulse. The highly energetic and spectrally quasi continuous cut-off XUV radiation may be separated by appropriate filters, producing isolated pulses with sub-femtosecond pulse duration [17, 18]. A crucial parameter in this generation mechanism is the relative phase between the carrier frequency and the envelope of the few-cycle pulse [19, 20], which determines the location of the highest amplitude cycle under the pulse envelope. The pulse-to-pulse reproducibility of the emission characteristics rely on the stabilization of this relative phase, and it has been achieved [21] recently also in amplified few cycle pulses [21].

In contrast to the stabilized few-cycle pulses, many cycle laser pulses excite a number of electron wave packets into the continuum, which following different trajectories recombine to give rise to the “plateau” harmonics. In this case from all the interfering quantum paths, two dominant trajectories remain, contributing to a given photon energy below the cut-off [22]. Their return times are less than a laser period but different, so one speaks of a “long” and a “short” trajectory. As far as the attosecond pulse generation is concerned, it is the total phase that the harmonic dipole moment accumulates during the motion of the electron in the continuum that plays a decisive role. Only if the phases of all spectral components in the frequency “comb” are “locked”, i.e., if the phase difference between neighbouring harmonics and within the spectral distribution of each harmonic is constant at any given time, spikes of attosecond duration would appear in the time-domain as a result of frequency beating. Additionally propagation conditions should further maintain phase locking.

In the quest for laboratory pulse trains, the diagnostics for the temporal characterization of attosecond pulse trains and isolated pulses up to now are based on cross-correlation measurements between the field of the fundamental and that of the XUV radiation. Cross correlation is a powerful tool in short optical pulse metrology. However, it is an indirect approach, based on appropriate modelling that correctly describes the cross-correlation process, which becomes rather complicated in the presence of the strong IR field. An important measurement of the relative phase between plateau harmonics based on a cross-correlation measurement has been recently reported [8]. In the well-established femtosecond metrology, the most widely used methods rely on a non-linear effect induced by the radiation to be characterized solely. The higher the degree of the non-linearity, the larger the number of the field parameters that can be deduced. But, even a second order autocorrelation (AC) is sensitive to the spectral phase distribution of the radiation to be analyzed, and thus its pulse duration can be determined to a satisfactory degree of accuracy. This is why second order AC has been the routinely used metrology tool in pico- and femtosecond

laser laboratories for many years. The extension of the approach to sub-femtosecond XUV pulses is far from trivial as attosecond pulses are necessarily in the UV-XUV spectral range, orders of magnitude weaker than the laser radiation and spectrally much broader. The wavelength region below 100 nm is notoriously the most difficult spectral region to handle experimentally. It is characterized by a complete lack of refractive optical components and even reflective optics are either of low reflectance or narrow bandwidth. The choice of an appropriate beam splitter in a conventional Michelson interferometer normally employed in auto-correlation measurement becomes an unsolvable problem. The fragile attosecond pulses require fully dispersionless optical arrangements. The non-linear detector has to rely on a two photon process, such as two photon ionization. The sensitivity of such a process is usually too low to produce measurable signal and given the broad harmonic spectrum, it should have a flat response for the wavelengths involved in the superposition. Those are the obstacles that prevented a successful measurement of a 2nd order AC of an attosecond pulse train or isolated pulse so far.

In the present work, we report on the progress towards a direct measurement of attosecond pulse trains emerging from a superposition of harmonics with a method that overcomes these stumbling blocks. Key factors towards this goal are (i) the technique of the volume auto-correlation to be employed in place of a beam splitter and (ii) the demonstration of the two-photon ionization process in helium as an appropriate detector [23]. The method can be extended to different spectral regions by an appropriate choice of the atomic (or ionic) medium for the two-photon ionization. Extension to isolated pulses is in principle possible, but upon substantial increase of the currently available XUV fluencies.

The mission of the recently initiated attoscience is to generate and characterize attosecond radiation pulses in order to use them in the investigation of ultrafast dynamical effects by means of pump-probe measurements [24]. Pump-probe experiments are based on non-linear effects; commonly a two photon absorption process. The method presented in this work relies on such a non-linear process and thus opens up the path to XUV-pump XUV-probe measurements at unprecedented short time scales.

## 2 Experimental set up

The experiments reported here have been performed at the ATLAS facility of the Max Planck Institut für Quantenoptik using a set up, which draws upon the apparatus used in our earlier investigations [23]. The main modification is that instead of a Kirckpatrick–Baez focusing system used in [23], we simply use a spherical gold mirror, cut into two halves for reasons explained in the next paragraph, with a 30 cm radius of curvature. The harmonic generation occurs in a xenon gas-jet using up to 10 mJ, 130 fs laser pulses at  $\lambda = 790$  nm from the 10 Hz Ti : Sapphire laser. The laser beam focus was 6 mm before the Xe gas jet, at a position that theoretical calculations predict optimum phase locking [25]. In order to reduce the amount of the fundamental after the xenon jet, an annular beam is used the inner part of which contains the harmonic emission and the outer part is blocked by an iris

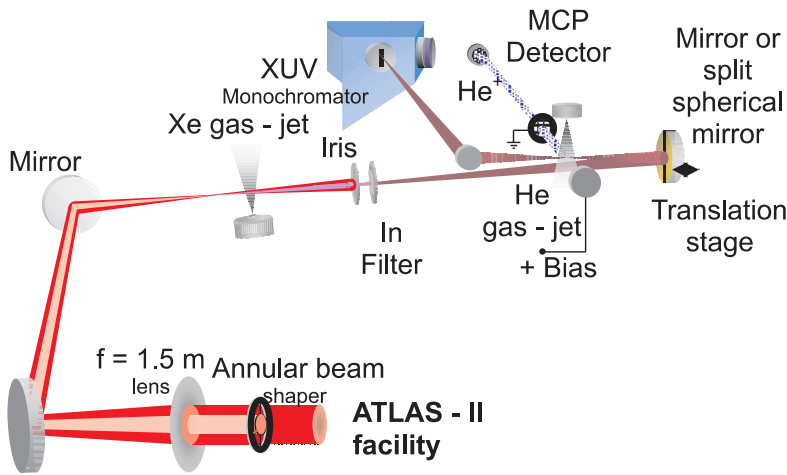


FIGURE 1 Experimental setup

after the Xe jet. For the laser intensities employed, harmonics of up to the 15th are generated. A  $0.2\ \mu\text{m}$  Indium filter selects practically a group of harmonics from the 7th to the 15th and suppresses further the fundamental. The XUV pulse radiation is focused in a second gas jet with helium and the harmonic radiation was recorded by a XUV monochromator coupled with the harmonic production chamber through a gold mirror with 60 cm radius of curvature. The ionization products are detected by a time-of-flight (TOF) mass spectrometer.

### 3 The broadband non-linear detector

As a non-linear broadband XUV detector can be used, the two-photon ionization of He is induced by the radiation to be characterized, namely the generated and transmitted by the In filter harmonic superposition. In Fig. 2 the harmonic spectrum is shown before (solid line) and after the In filter (dashed line). After correction for the reflectivity of the gold mirror and the efficiency of the spectrograph and detector, the relative intensity amplitude is  $7 : 9 : 11 : 13 : 15 : 0.34 : 1.0 : 0.25 : 0.11 : 0.01$ . It is worth mentioning that despite the small number of harmonics in the “comb” under investigation and the unequal amplitudes, an ideal phase-locking of these harmonics (all phases equal to zero) would produce an attosecond train with Full-Width-Half-Maximum (FWHM) “wagons” duration of  $\tau_{\text{XUV}} = 335$  as (see lower panel in Fig. 2). This is relatively close to the Fourier transform-limited value  $\tau_{\text{XUV}} = T_L/2N = 263$  as for the duration of each subcycle pulse as determined by  $N = 4$  harmonics of equal amplitude in a superposition. This indicates the relative low sensitivity of the pulse duration on the relative amplitudes of the harmonics. The combination of He as ionization medium and In as filter material for the selection of a group of harmonics possesses several advantages. This becomes clear if one considers the possible ionization channels by the available harmonics in relation to the ionization potential (IP) of 24.6 eV for He (see Fig. 3a). On the high frequency side, only harmonics higher than the 15th (17th, 19th, ...) can give rise to single photon ionization. The harmonics in the transmitted superposition can induce only two-photon ionization, either by two photons of the same energy (with the exemption of the 7th harmonic) or by any combination of the photon energies in the superposition. The

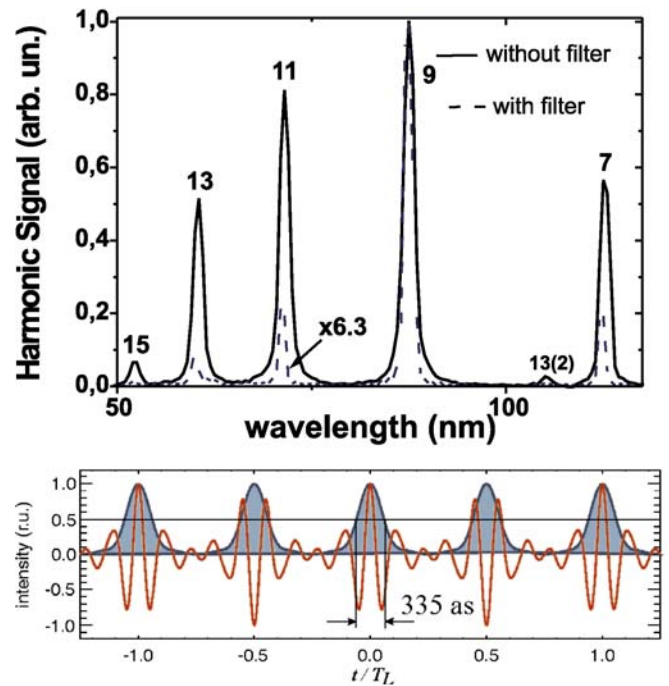


FIGURE 2 Higher order harmonic generation spectra produced in the Xe jet as measured without the In filter (solid line) and transmitted through the In filter (dashed line). The lower panel shows the electric field amplitude (red line) and the instantaneous intensity (blue line) of the superposition of these harmonics, after correction of the transmitted intensities for the reflectivity of the gold mirror and the efficiency of the XUV spectrometer and detector, assuming zero initial phases for all of them

properties of this non-linear detector have been investigated in detail in a previous experiment and the yields for the same harmonic superposition calculated numerically solving the Time Dependent Schrödinger Equation (TDSE) for He in a polychromatic laser field [23]. These calculations have revealed the flatness of the response of the detector at the frequency intervals of interest. The maximum variation of the response for the entire wavelengths of interest is by a factor of two. This variation may affect the measured duration in a second order autocorrelation measurement, effectively increasing it by a factor of a few percent, an acceptable systematic error. Because, it is difficult to ascertain a priori whether the 17th harmonic is sufficiently suppressed as not to cause single pho-

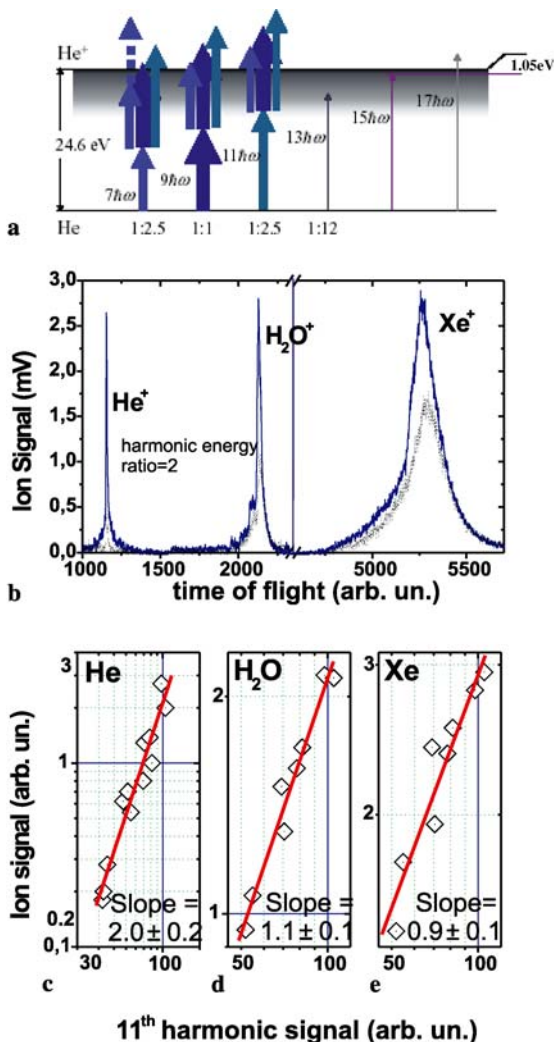


FIGURE 3 Ionization scheme (a); Measured ion mass time of flight spectrum for two harmonic energies (b); XUV intensity dependencies of He<sup>+</sup> (c), H<sub>2</sub>O<sup>+</sup> (d) and Xe<sup>+</sup> (e)

ton ionization, we have performed measurements with the present experimental setup with ion yield versus harmonic intensity for three ions (He<sup>+</sup>, H<sub>2</sub>O<sup>+</sup>, and Xe<sup>+</sup>). Figure 3e, shows two typical TOF mass spectra produced by the harmonic superposition at two different energies. Xe atoms originate from the harmonic generation jet, while water molecules appearing in the spectrum are rest gas molecules of the chamber. The lower three graphs give the ion yield variation as a function of the 11<sup>th</sup> harmonic intensity for the He<sup>+</sup> (c), for H<sub>2</sub>O<sup>+</sup> (d), and Xe<sup>+</sup> (e) ions. The fact that the intensity dependence for He<sup>+</sup> (IP = 24.6 eV) is very nearly quadratic while for H<sub>2</sub>O<sup>+</sup> (IP = 12.6 eV), and Xe<sup>+</sup> (IP = 12.1 eV) linear provides clear evidence that the influence of the 17<sup>th</sup> harmonic is negligible and that the He<sup>+</sup> ionization signal is due to a two-photon absorption and thus is ideally suited for a second-order autocorrelation measurement.

#### 4 A non-linear autocorrelation technique

The above described set up can be used for a second-order autocorrelation measurement if one of the

halves of the spherical mirror would be movable by means of a piezoelectric translation stage. The mirror would act then as a wavefront splitting arrangement [26] appropriate for non-linear autocorrelation measurements. With such a mirror, the measured signal of the He<sup>+</sup> ions will result from the two-photon absorption from the coherent superposition of the two replicas of the attosecond train. Assuming that the generated XUV radiation has cylindrical symmetry, we can represent a second order AC measurement.

There are two points that distinguish this technique from the conventional Michelson interferometer based on a non-linear crystal or a non-linear photodiode. (a) The signal produced stems from the interaction of the pulse within a volume defined by the focusing properties of the spherical mirror and not from a plane, as in the case of a non-linear crystal commonly used in non-linear autocorrelators for fs pulses. (b) Unlike the amplitude splitting arrangements, the split mirror technique is a wavefront splitting device and, as such, a delay variation results not in a change of the energy reaching the detector, but simply in a spatial redistribution of the energy in the focal volume according to the diffraction principle.

For a given wavelength  $\lambda$ , a certain displacement of  $D$  between the two half mirrors has the effect of modifying the intensity distribution of the focal spot for zero displacement (Airy spot). Since the total energy in the interaction volume is conserved for all relative delays. In the case of a linear detector, the signal for every delay would be the same and no modulation of the signal with the relative delay would be observed. For a non-linear detector, however, the rearrangement of the local intensity inside the interaction volume would introduce a modulation in the measured signal. For a harmonic superposition, the intensity distributions are expected to become much more complicated but the principle remains the same.

#### 5 Conclusion

For a quantitative analysis of second order autocorrelation traces a thorough understanding of this autocorrelation technique is necessary. This study has been finalized and will be presented elsewhere [27]. The main result of this study is that for an intensity autocorrelation trace, the peak to background ratio is reduced as compared to that of a conventional autocorrelator, but high enough to observe a modulated signal from which the mean value of the attosecond pulse train “wagons” can be extracted. Applying this technique to the above mentioned superposition of the 7<sup>th</sup>–15<sup>th</sup> harmonics, we have obtained very promising results, which will be presented elsewhere [27].

It is worth noting that the presented approach demonstrates the feasibility of temporal measurements utilizing a non-linear effect in the He atom that has a fairly low non-linear susceptibility. As such, it at the same time reveals the feasibility of and opens up the path to XUV-pump XUV-probe type of time domain applications of attosecond pulses to other gas phase or solid state systems.

The 2<sup>nd</sup> order autocorrelation measurement, once established as an attosecond metrology tool, can be extended, by employing energy resolved photoelectron spectroscopy instead of mass spectroscopy, to a second order frequency

resolved XUV Gating [28]. These will be the near future developments, complementary to the cross-correlation SPIDER [29] or FROG type [30] approaches, in attosecond pulse metrology

**ACKNOWLEDGEMENTS** Two of us (D.C. and N.A.P.) would like to thank the Max-Planck-Institute für Quantenoptik Plasma Group for the assistance and hospitality during their stay in Garching. This work is supported in part by the European Community's Human Potential Programme under contract CT-HPRN-2000-00133 (ATTO) and the Ultraviolet Laser Facility (ULF) (contract no. HPRI-1999-CT-00074).

## REFERENCES

- 1 G. Steinmeyer, D. Sutter, L. Gallmann, N. Matuschek, U. Keller: *Science* **286**, 1507 (1999)
- 2 T.W. Hänsch: *Opt. Commun.* **80**, 71 (1990)
- 3 Gy. Farkas, Cs. Tóth: *Phys. Lett. A* **168**, 447 (1992)
- 4 S.E. Harris, J.J. Macklin, T.W. Hänsch: *Opt. Commun.* **100**, 487 (1993)
- 5 I.P. Christov, M.M. Murnane, H. Kapteyn: *Phys. Rev. Lett.* **78**, 1251 (1997)
- 6 M. Hentschel, R. Kienberger, C. Spielmann, G.A. Reider, N. Miloevic, T. Brabec, P. Corkum, U. Heinzmann, M. Drescher, F. Krausz: *Nature* **414**, 509-513 (2001)
- 7 N.A. Papadogiannis, B. Witzel, C. Kalpouzos, D. Charalambidis: *Phys. Rev. Lett.* **83**, 4289 (1999)
- 8 P.M. Paul, E.S. Toma, P. Breger, G. Mullot, F. Augé, Ph. Balcou, H.G. Muller, P. Agostini: *Science* **292**, 1689 (2001); H.G. Muller: *Appl. Phys. B* **74** [Suppl.], 17 (2002)
- 9 P.B. Corkum: *Phys. Rev. Lett.* **71**, 1995 (1993)
- 10 M. Lewenstein, Ph. Balcou, M.Yu. Ivanov, A. L'Huillier, P.B. Corkum: *Phys. Rev. A* **49**, 2117 (1994)
- 11 P. Salières et al.: *Science* **292**, 902 (2001)
- 12 A. Baltuška et al.: *Appl. Phys. B* **65**, 175 (1997)
- 13 M. Nisoli et al.: *Appl. Phys. B* **65**, 189 (1997)
- 14 U. Morgner et al.: *Opt. Lett.* **24**, 411 (1999)
- 15 D.H. Sutter et al.: *Opt. Lett.* **24**, 631 (1999)
- 16 A. Shirakawa et al.: *Appl. Phys. Lett.* **74**, 2268 (1999)
- 17 T. Brabec, F. Krausz: *Rev. Mod. Phys.* **72**, 545 (2000)
- 18 R. Kienberger, M. Hentschel, M. Uiberacker, Ch. Spielmann, M. Kitzler, A. Scrinzi, M. Wieland, Th. Westerwalbesloh, U. Kleineberg, U. Heinzmann, M. Drescher, F. Krausz: *Science* **297**, 1144 (2002)
- 19 G.G. Paulus et al.: *Nature* **414**, 182-184 (2001)
- 20 D.J. Jones, S.A. Diddams, J.K. Ranka, A. Stentz, R.S. Windeler, J.L. Hall, S.T. Cundiff: *Science* **288**, 635 (2000)
- 21 A. Baltuška, Th. Udem, M. Uiberacker, M. Hentschel, E. Goulielmakis, Ch. Gohle, R. Holzwarth, V. Yakovlev, A. Scrinzi, T.W. Hänsch, F. Krausz: *Nature* **421**, 611-615 (2003)
- 22 Ph. Antoine, A. L'Huillier, M. Lewenstein: *Phys. Rev. Lett.* **77**, 1234 (1996)
- 23 N.A. Papadogiannis, L.A.A. Nikolopoulos, D. Charalambidis, P. Tzallas, G. Tsakiris, K. Witte: *Phys. Rev. Lett.* **90**, 133902 (2003); N.A. Papadogiannis, L.A.A. Nikolopoulos, D. Charalambidis, G.D. Tsakiris, P. Tzallas, K. Witte: *Appl. Phys. B* **76**, 721 (2003)
- 24 M. Drescher, M. Hentschel, R. Kienberger, M. Uiberacker, V. Yakovlev, A. Scrinzi, T. Westerwalbesloh, U. Kleineberg, U. Heinzmann, F. Krausz: *Nature* **419**, 803 (2002)
- 25 M.B. Gaarde, K.J. Schafer: *Phys. Rev. Lett.* **89**, 213901 (2002)
- 26 E. Constant, E. Mével, A. Zaïr, V. Bagnoud, F. Salin: *J. Phys. IV Fr.* **11**, Pr2-537 (2001)
- 27 P. Tzallas, D. Charalambidis, N.A. Papadogiannis, K. Witte, G.D. Tsakiris: *Nature* **426**, 267 (2003)
- 28 T. Sekikawa, T. Katsura, S. Miura, S. Watanabe: *Phys. Rev. Lett.* **88**, 193902 (2002)
- 29 F. Quéré, J. Itatani, G.L. Yudin, P.B. Corkum: *Phys. Rev. Lett.* **90**, 073902 (2003).
- 30 J. Norin, et al.: *Phys. Rev. Lett.* **88**, 193901 (2002)